J Biol Inorg Chem (2010) 15:259–269
DOI 10.1007/s00775-009-0594-5

ORIGINAL PAPER

Tumor cellular proteasome inhibition and growth suppression by 8-hydroxyquinoline and clioquinol requires their capabilities to bind copper and transport copper into cells

Shumei Zhai · Lei Yang · Qiuzhi Cindy Cui · Ying Sun · Q. Ping Dou · Bing Yan

Received: 1 July 2009 / Accepted: 26 August 2009 / Published online: 7 October 2009
© SBIC 2009

Abstract We have previously reported that when mixed with copper, 8-hydroxyquinoline (8-OHQ) and its analog clioquinol (CQ) inhibited the proteasomal activity and proliferation in cultured human cancer cells. CQ treatment of high-copper-containing human tumor xenografts also caused cancer suppression, associated with proteasome inhibition in vivo. However, the nature of the copper dependence of these events has not been elucidated experimentally. In the current study, using chemical probe molecules that mimic the structures of 8-OHQ and CQ, but have no copper-binding capability, we dissected the complex cellular processes elicited by 8-OHQ–Cu and CQ–Cu mixtures and revealed that copper binding to 8-OHQ or CQ is required for transportation of the copper complex into human breast cancer cells and the consequent proteasome-inhibitory, growth-suppressive, and apoptosis-inducing activities. In contrast, the non-copper-binding analogs of 8-OHQ or CQ blocked the very first step—copper binding—in this chain of events mediated by 8-OHQ–Cu or CQ–Cu.

Keywords Copper-dependence · Clioquinol · Breast cancer · Chemical probe · Chemical biology

Electronic supplementary material The online version of this article (doi:10.1007/s00775-009-0594-5) contains supplementary material, which is available to authorized users.

S. Zhai · Y. Sun · B. Yan
School of Chemistry and Chemical Engineering, Shandong University, Jinan, China

S. Zhai · Q. C. Cui · Q. P. Dou (✉)
The Prevention Program, Barbara Ann Karmanos Cancer Institute, and Department of Pathology, School of Medicine, Wayne State University, 540.1 HWCRC, 4100 John R Road, Detroit, MI 48201, USA
e-mail: doup@karmanos.org

L. Yang · B. Yan (✉)
Department of Chemical Biology and Therapeutics, St. Jude Children's Research Hospital, 262 Danny Thomas Place, Memphis, TN 38105, USA
e-mail: bing.yan@stjude.org

Introduction

Copper is an essential cofactor for many enzymes and a key one electron transfer reaction donor involved in reactive oxygen species generation. Therefore, the concentration of copper in organisms is tightly regulated [1, 2]. However, copper concentration is elevated in cancerous tissues of breast, prostate, lung, and brain [3–6]. The detailed molecular mechanisms for this cancer-associated copper elevation are not clear. Regardless of that, the vital role of copper in angiogenesis, a process critical for tumor growth, has been well documented [7–9]. Because the copper level elevation is cancer-specific, copper-targeting agents can be developed as more selective anticancer therapeutics [10]. The strong copper chelator tetrathiomolybdate was shown to stabilize kidney cancer [11, 12]. However, the cancer kept advancing in patients before the copper concentration was significantly lowered, suggesting that just passively eliminating free copper is not enough.

The ubiquitin–proteasome pathway is essential for the cell cycle, apoptosis, angiogenesis, and differentiation [13, 14]. This pathway contributes to the pathological state of several human diseases, including cancer, in which some regulatory proteins are either stabilized owing to decreased degradation or lost owing to accelerated degradation [15]. The 20S proteasome, the proteolytic core of the 26S

proteasome complex, contains multiple peptidase activities, including the chymotrypsin (CT)-like, trypsin-like, and peptidylglutamyl peptide hydrolyzing like activities [16]. It has been reported that all three types of activities contributed significantly to protein breakdown and their relative importance varied widely with the substrate [17]. However, only the inhibition of the CT-like but not other proteasomal activities is a strong stimulus that induces apoptosis [18, 19].

8-Hydroxyquinoline (**1**; Fig. 1) is a monoprotic bidentate chelating agent. Previous studies have shown that **1** and some of its derivatives exhibited substantial cytotoxic activity against cancer cells [20, 21]. The bis(8-hydroxyquinoline)-substituted benzylamine derivatives are more efficient than the monohydroxyquinoline analogs in their antitumor activities [22] and in the inhibition of the precipitation of Aβ peptides induced by Cu^{2+} and Zn^{2+} in Alzheimer disease [23]. Others reported that **1** is more active than its substituted quinoline analogs in the differentiation-inducing effect in the MCF-7 human breast cancer cell [24].

We and others have previously reported that **1**, clioquinol (**4**; Fig. 1), and some other analogs could bind copper in solution [25–30]. The X-ray crystal structures of copper complexes or structural models have also been reported [31–33]. These ligand–copper mixtures inhibited the proteasome and superoxide dismutase-1 activities, resulting in proliferation suppression and apoptosis inducement in cultured cancer cells, and **4** also inhibited tumor growth in a xenograft mice model [27, 29]. It was found that **4** can act therapeutically by changing the distribution of copper or facilitating copper uptake in yeast cells [34]. Another report showed that **4** inhibited the proteasome and induced cell death primarily through a copper-dependent mechanism, displaying preclinical activity in leukemia and myeloma [35]. These results suggested that the chelation of copper or changes in cellular copper may be required for the anticancer activities of **1** and **4**, although this speculation has not been proven through experiments.

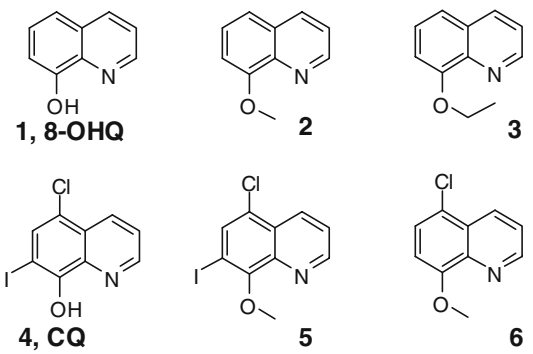

Fig. 1 Structures of 8-hydroxyquinoline (*8-OHQ*), clioquinol (*CQ*), and some analogs

However, copper-independent growth-inhibitory activities were also reported, such as the ability of clioquinol to upregulate PI3K and inhibit p53 activity [36]. Since copper ions are always present in cells, these observations could not completely exclude the possibility of **4**–copper complex formation. To clarify the role of copper chelation in the anticancer activities of **1** and **4**, we investigated the enzymatic and cellular activities of their close analogs (8-methoxyquinoline, **2**; 8-ethoxyquinoline, **3**; 5-chloro-7-iodo-8-methoxyquinoline, **5**; 5-chloro-8-methoxyquinoline, **6**; Fig. 1) that lacked copper-binding abilities. We found that in contrast to **1** and **4**, which could enhance the cellular copper uptake, their non-copper-binding derivatives failed to do so. Furthermore, different from **1** and **4**, the non-copper-binding compounds **2**, **3**, **5**, and **6** could neither inhibit the CT-like activity of the proteasome in human breast cancer cell cultures nor induce cancer cell death. Our results demonstrate that copper binding and cell uptake of copper are required for the proteasome-inhibitory and growth-suppressive activities of **1** and **4** in human breast cancer cells.

Results

Synthesis and characterization of analogs of 1 and 4

The main hypothesis of this investigation is that we can test the role of copper binding by **1** and **4** in proteasome and cancer cell inhibition by investigating their analogs that maintain a similar molecular structure without copper-binding capability. For this purpose, we synthesized and/or acquired compounds **1**–**6** (Fig. 1). Compounds **2** and **3** have a structure similar to that of **1**, but their 8-hydroxyl group, which is crucial for copper chelating [37], is blocked. Compounds **5** and **6** are mimics of **4** without copper-binding capability. These compounds were purified by chromatographic methods and their structures and purities were confirmed by liquid chromatography (LC)–mass spectrometry (MS) and ^{1}H NMR methods.

Binding constant of copper–ligand determined by UV–vis titration

Both **1** and **4** bind to copper and form complexes. The UV absorption maxima of **1** and **4** at approximately 250 nm were shifted to approximately 275 nm upon copper binding (Fig. 2a, d), indicating the formation of a copper complex. Previous reports indicated that they were 2:1 (ligand to copper) complexes and that **4**–Cu has a stability constant of 2×10^{10} [37, 38]. However, compounds **2**, **3**, **5**, and **6** could not form complexes with copper (Fig. 2b, c, e, f) in the physiologically achievable concentration range.

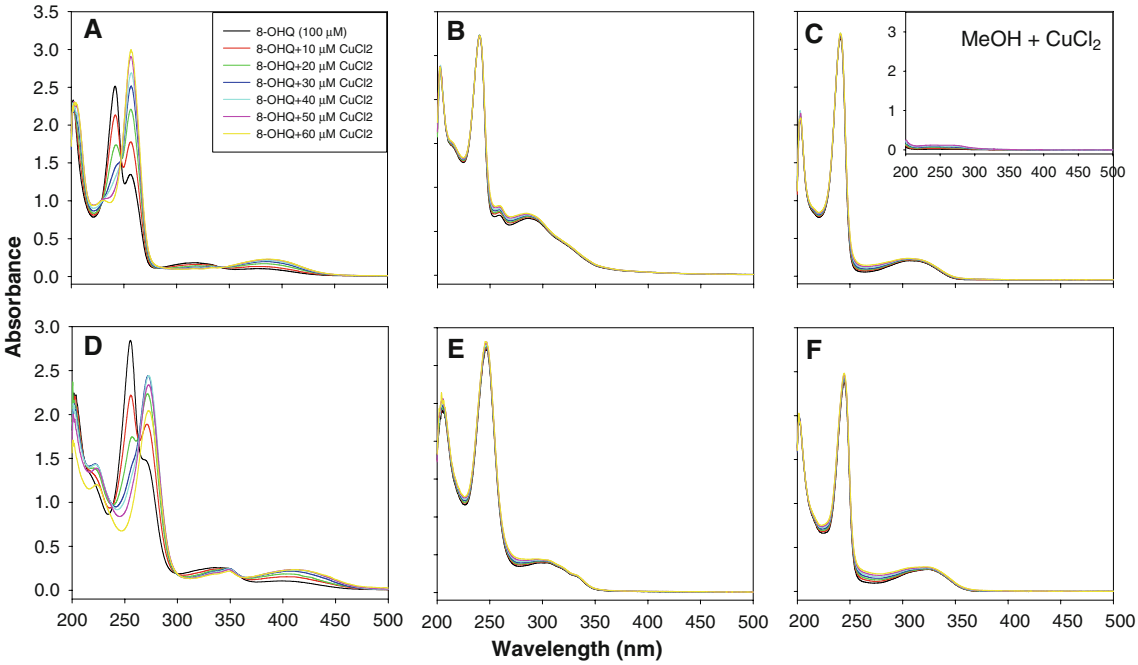

Fig. 2 UV–vis titration of the binding between **4** (**a**), **1** (**d**), or analogs (**b**, **c**, **e**, **f**) and $CuCl_2$ in methanol solution. A 0.1 mM methanol solution of each compound was titrated with different amounts of $CuCl_2$ methanol solution (2.5 mM)

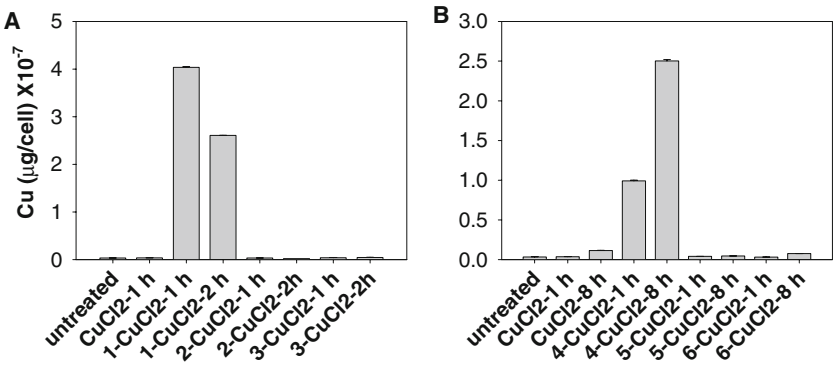

Fig. 3 Effect of compound–copper mixtures on cellular copper uptake in human breast cancer MCF10DCIS.com (DCIS) cells. Cells were treated with 10 μM compound–copper mixtures for the time periods indicated. Then cells were collected and the copper accumulation in cells was quantitatively measured by inductively coupled plasma optical emission spectroscopy

1 and **4**, but not their non-copper-binding analogs, can facilitate transport of copper into cells

To investigate the relationship between the amount of cellular copper and the copper-binding ability of **1**–**6**, we determined the amount of cellular copper after incubation with each compound–copper mixture. Human breast cancer cell line MCF10DCIS.com (DCIS) cells were treated with 10 μM concentrations of each mixture for 1, 2, or 8 h, and the cells were collected and dissolved in nitric acid for measurement of the copper content by inductively coupled plasma optical emission spectroscopy (ICP-OES). The effects of the compound–copper mixture on cellular copper accumulation are shown in Fig. 3. The amount of copper in untreated DCIS cells was 0.03×10^{-7} μg/cell. When cells were treated with mixtures of **1**–$CuCl_2$, **2**-$CuCl_2$, and **3**–$CuCl_2$ at 10.0 μM for 1 h, the levels of cellular copper were found to be 4.04×10^{-7}, 0.03×10^{-7}, and 0.04×10^{-7} μg/cell, respectively (Fig. 3a), corresponding to at least 100-fold difference in the ability to accumulate cellular copper between **1** and its inactive analogs **2** and **3**. Similar results were obtained for **4** and its inactive analogs. The accumulation of copper in DCIS cells treated for 8 h with **4**–$CuCl_2$, **5**–$CuCl_2$, and **6**–$CuCl_2$ were 2.50×10^{-7}, 0.05×10^{-7}, and 0.07×10^{-7} μg/cell, respectively (Fig. 3b), representing a 40–50-fold difference. These data showed a close correlation between the copper-binding ability of compounds and the cell uptake of copper.

To study whether the failure of the copper mixtures of inactive analogs of **1** and **4** to accumulate cellular copper content (Fig. 3) was due to the failure of these analogs to enter cells, we performed a parallel artificial membrane

Table 1 Caco-2 and parallel artificial membrane permeability assay (*PAMPA*) results

Compound	Caco-2 Papp A→B (nm/s)	Caco-2 Papp B→A (nm/s)	Caco-2 efflux ratio	PAMPA Pe ($\times 10^{-6}$ cm/s)
1	380 ± 148	290 ± 11	0.8	213 ± 16
2	483 ± 26	299 ± 7	0.6	682 ± 109
3	207 ± 146	94 ± 25	0.5	726 ± 248
4	473 ± 61	315 ± 22	0.7	334 ± 31
5	215 ± 31	125 ± 16	0.6	779 ± 54
6	604 ± 24	413 ± 27	0.7	308 ± 49

See Fig. 1 for the structures of the compounds.

Papp apparent permeability coefficient, *A* apical side, *B* basolateral side, *Pe* effective permeability

permeability assay (PAMPA) and a Caco-2 membrane permeability assay and evaluated the membrane permeability of **1**–**6**. We found that the permeabilities of all six compounds in these different assays are highly comparable (Table 1). Therefore, the failure of the non-copper-binding analogs of **1** and **4** to accumulate cellular copper should be due to their inability to bind to copper and to transport copper into cells.

We realized that a ligand alone could also have an effect on copper detoxification; therefore, the effects of **1** and **4** as well as their non-copper-binding analogs on copper detoxification should also be studied in the future.

1 and 4, but not their non-copper-binding analogs, can inhibit breast cancer cell growth

We have reported previously that a mixture of **1** or **4** and copper selectively inhibited proliferation and induced apoptosis in malignant breast cells [28, 32]. To investigate the relationship between the antiproliferative activity of compounds **1**–**6** and their copper-binding property and capability to enhance cell uptake of copper, we studied the effects of compound–$CuCl_2$ mixtures on cell growth.

Human breast cancer DCIS cells were treated with active **1** and **4** as well as their non-copper-binding counterparts (**2**, **3**, **5**, and **6**), followed by observation of cellular morphological changes and performance of the 3-(4,5-dimethyltiazol-2-yl)-2.5-diphenyltetrazolium bromide (MTT) assay. After even 1-h treatment, **1** but not its analogs (**2** and **3**) caused the cells to round up and become detached (Fig. 4a). Similarly, an 8-h treatment with **4** but not its inactive analogs (**5** and **6**) caused the apoptotic morphological changes (Fig. 4a). Furthermore, the cellular morphological changes correlated well with the growth-inhibitory activities of these copper–compound mixtures. When DCIS cells were treated with various concentrations of each mixture for 24 h, copper-

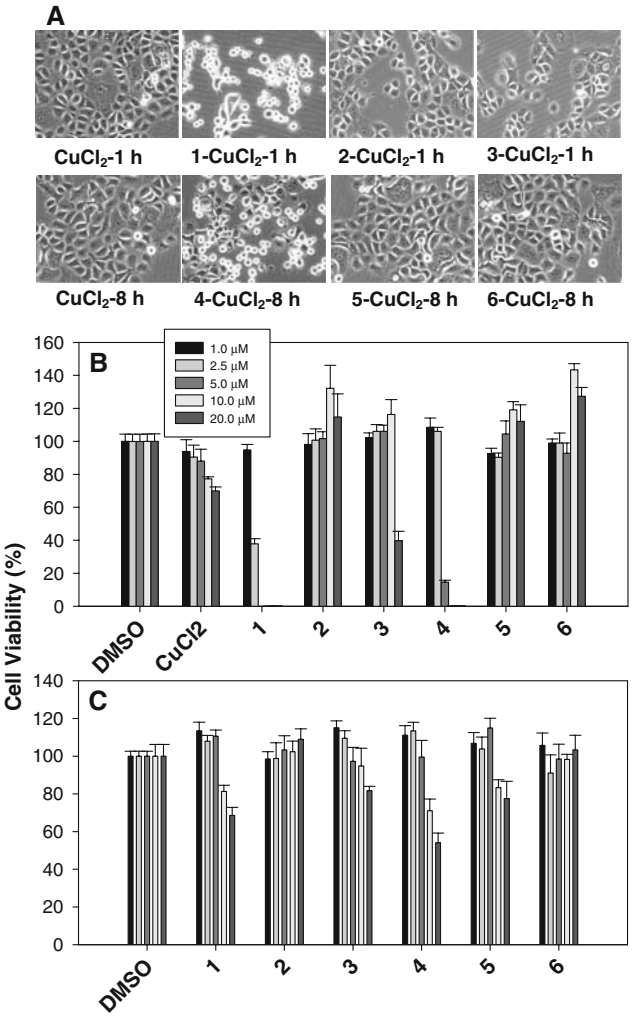

Fig. 4 The antiproliferative effect of the compound–copper mixtures. Cell morphological changes in the DCIS cells treated with 10 μM compound–copper mixtures for the time periods indicated (**a**). Cell viabilities were measured after 24-h treatment with compound–$CuCl_2$ (**b**) or with the compound alone (**c**) at different concentrations. After the medium had been removed, viable cells were analyzed by the 3-(4,5-dimethyltiazol-2-yl)-2.5-diphenyltetrazolium bromide method. Data (mean ± standard deviation, $n = 4$) are expressed as a percentage of viable cells in dimethyl sulfoxide (*DMSO*) treatment

containing mixtures of **2**, **3**, **5**, and **6** had much less growth-inhibitory effect in contrast to that of **1**–$CuCl_2$ and **4**–$CuCl_2$ (Fig. 4b). **2**–$CuCl_2$ had no effect on cell proliferation at all the concentrations tested, **3**–$CuCl_2$ inhibited cell proliferation by approximately 60% at 20 μM, whereas **1**–$CuCl_2$ caused approximately 60% inhibition even at 2.5 μM (Fig. 4b). Copper mixtures of **5** and **6** could not inhibit cell growth even at the highest concentration used (20 μM) (Fig. 4b). In contrast, **4**–$CuCl_2$ caused approximately 85% inhibition even at 5.0 μM (Fig. 4b). The compounds alone, including **1** and **4**, showed much less or no toxicity under the same conditions (Fig. 4c). Therefore, these data show

that copper-dependent inhibition of cell proliferation by active compounds is related to their copper-binding capability.

1–Cu and 4–Cu, but not mixtures of their analogs and copper, could induce cancer cell death in a concentration- and time-dependent manner

Compounds **1** and **4** have some toxicity in DCIS cells. However, their toxicity was greatly enhanced when **1**–Cu or **4**–Cu was used. Such copper dependence was studied using both morphological examination and a cell proliferation assay (Fig. 4b). DCIS cells were treated with mixtures of **1**–**6** and $CuCl_2$ at various concentrations for 12 h. After treatment, the cell morphology was observed under microscope (Fig. 5a, b). Treatment of DCIS cells with **1**–$CuCl_2$ and **4**–$CuCl_2$ mixtures resulted in a time- and concentration-dependent cytotoxicity (Fig. 5a, b; see also the electronic supplementary material), whereas **2**–$CuCl_2$ and **5**-$CuCl_2$ mixtures and the compound alone did not affect cell growth (Fig. 5a, b). After treatment with **1**–$CuCl_2$ and **4**-$CuCl_2$, the cell-death-related, calpain-mediated poly(ADP-ribose) polymerase (PARP) cleavage fragment p65 appeared in a time-dependent manner (Fig. 5c) [39]. In contrast, **2**–$CuCl_2$ and **5**-$CuCl_2$ mixtures had no obvious activity on inducement of cell death (Fig. 5; see also the electronic supplementary material).

Proteasome inhibition before cell death by 1–Cu or 4–Cu mixtures, but not their analogs

To ascertain the requirement of copper binding for proteasome-inhibitory activity of compounds **1** and **4**, we performed a time-dependent study. DCIS cells were treated with the copper mixtures of **1**, **2**, **4**, and **5** for various times. Cells were harvested and lysed. Proteasome inhibition was measured by levels of the CT-like activity, ubiquitinated proteins, and the proteasome target protein Bax.

The results from the activity assay showed that the **1**–$CuCl_2$ mixture inhibited the CT-like activity in a concentration- and time-dependent manner (Fig. 6a–d). We

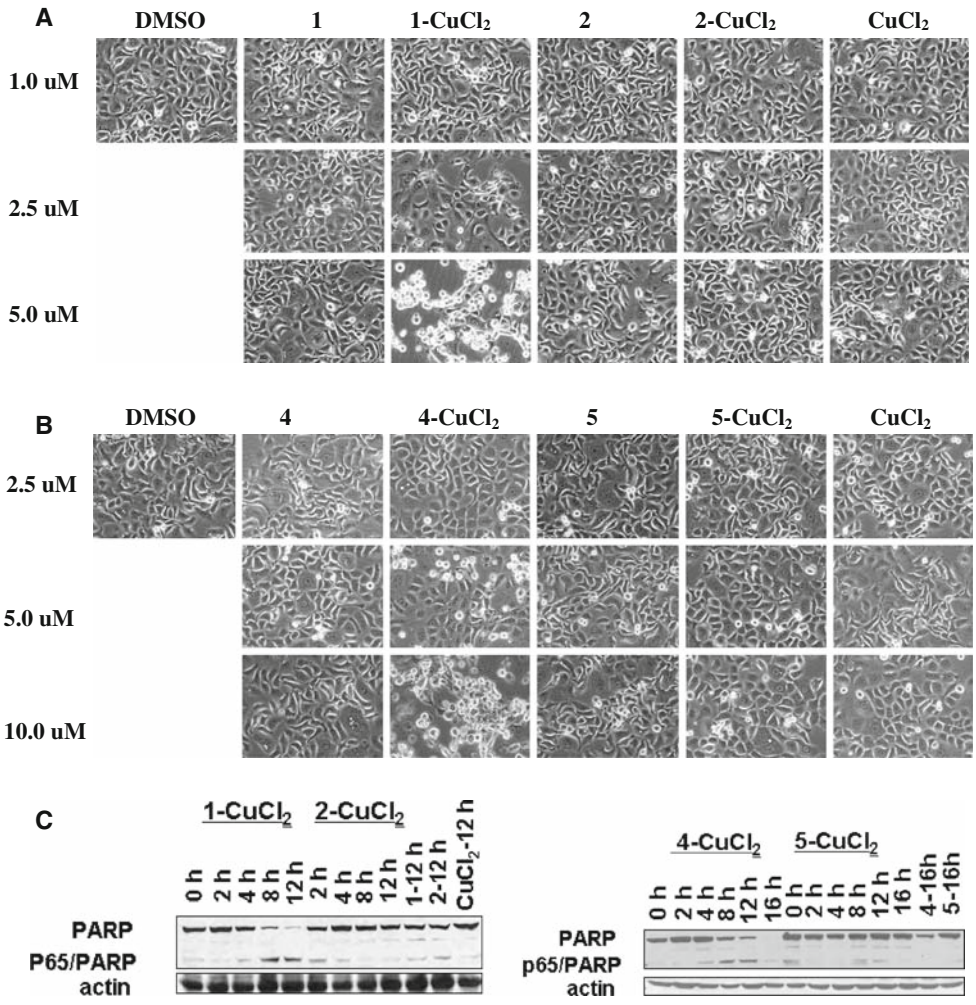

Fig. 5 Dose-dependent inducement of cell death in DCIS cells by **1**, **4**, and their analogs. Cell morphological changes in the DCIS cells treated with compounds **1**, **2**, **4**, and **5**, $CuCl_2$, or compound–Cu mixtures at increasing concentrations for 12 h (**a**, **b**). Time-dependent poly(ADP-ribose) polymerase (*PARP*) cleavage after treatment with $CuCl_2$ mixtures of **1**, **2**, **4**, and **5** is also shown (**c**)

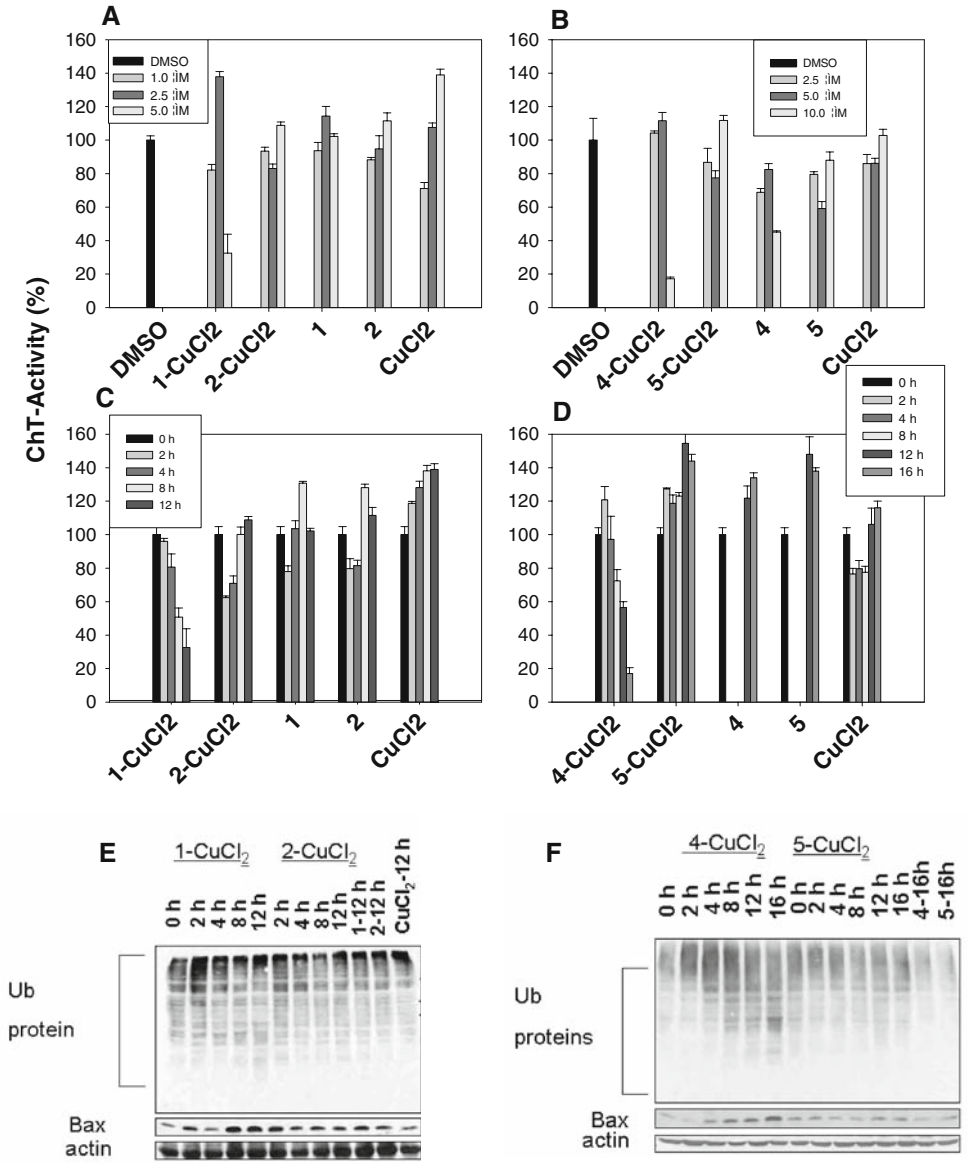

Fig. 6 Inhibition of proteasomal chymotrypsin-like activity by **1**–$CuCl_2$, **2**–$CuCl_2$, **4**–$CuCl_2$, and **5**–$CuCl_2$ mixtures. DCIS cells were treated with either solvent alone (DMSO) or with **1**–$CuCl_2$, **2**–$CuCl_2$, **4**-$CuCl_2$, and **5**–$CuCl_2$ mixtures at various concentrations (**a**, **b**) or for different time periods (**c**, **d**), followed by harvesting of cells to measure the proteasomal chymotrypsin-like activity (**a**–**d**), accumulation of ubiquitinated proteins, and accumulation of Bax protein (**e**, **f**). *ChT* chymotrypsin, *Ub* ubiquitinated

detected an approximately 20% inhibition of the proteasomal CT-like activity by the **1**–$CuCl_2$ mixture after 4 h of treatment, approximately 50% inhibition after 8 h, and approximately 67% inhibition after 12 h (Fig. 6c). In contrast, **2**–$CuCl_2$ did not show obvious inhibition of proteasomal CT-like activity. Similarly, an approximately 28% inhibition of the proteasomal CT-like activity by the **4**–$CuCl_2$ mixture after 8 h of treatment, approximately 44% inhibition after 12 h, and approximately 83% inhibition after 16 h were observed (Fig. 6d). The **5**–$CuCl_2$ mixture did not inhibit proteasomal CT-like activity. Consistent with decreased proteasomal activity, ubquitinated proteins and Bax also accumulated in a time-dependent manner as a resulted of treatment with mixtures of **1**–$CuCl_2$ or **4**–$CuCl_2$, but not **2**–$CuCl_2$ or **5**–$CuCl_2$ (Fig. 6e, f). For cells treated with the **1**–$CuCl_2$ mixture, both CT-like and trypsin-like activity (data not shown) were inhibited, leading to the accumulation of ubquitinated protein. When cells were treated with the **4**–$CuCl_2$ mixture, they were not inhibited in the same way (data not shown). This might explain the apparent discrepancy in the ubquitinated protein accumulation (Fig. 6e, f). Alternatively, these copper complexes might have multiple targets, including 20S and 19S proteasomes; the JAMM domain of the 19S caps in the 26S proteasome could be another possible target for these complexes and further studies are needed to assess this possibility [40].

Taken together, our data strongly suggest that tumor cellular proteasome inhibition and growth suppression by **1** and **4** requires their capabilities to bind copper and transport copper into cells.

Discussion

Copper is a crucial cofactor for a variety of cellular processes, such as respiration, iron homeostasis, antioxidant defense, angiogenesis, and immune responses. Now it has become very clear that the cellular and organ levels of copper ions are tightly regulated [1]. Many tumor tissues have the tendency to accumulate high concentrations of copper and copper is required in tumor development because of its role in angiogenesis. Therefore, the idea to convert cancer-promoting copper into a cancer-inhibiting drug is very attractive.

The ubiquitin–proteasome pathway plays a critical role in degradation of proteins that regulate cell cycle progression, proliferation, apoptosis, and angiogenesis [13, 14]. We have previously found that copper-binding compounds such as **1** and **4**, when mixed with copper, can inhibit the proteasome activity and induce apoptosis in cancer cells [28, 29, 32, 33]. Although this copper-dependent anticancer activity has been repeatedly reported, the nature of such dependence has not been experimentally elucidated. Several papers also reported copper-independent cancer cell growth inhibition, adding controversies and complications to this research area. In this investigation, we applied small chemical probe molecules to dissect the complex chemical and biological processes to gain a thorough understanding of the copper-dependent proteasome inhibition, cell death induction, and inhibition of cancer cell proliferation by **1** and **4**.

The chemical probe molecules **2**, **3**, **5**, and **6** maintain the overall structural skeletons of **1** and **4**, but do not have the copper-binding capability. They provide ideal tool molecules to investigate the role of copper binding in this complicated cellular process triggered by **1** and **4** without altering the molecular interactions with numerous cellular components that **1** and **4** have.

The first finding is that the strong copper-binding capabilities by **1** and **4** in combination with their superb membrane permeability transported a large amount of copper into cells, most likely still in the form of **1**–Cu or **4**–Cu complexes. Analogs that did not bind copper lost such activity, although the analog molecules themselves were expected to still accumulate inside cells owing to their excellent cell membrane permeability (Table 1). In the presence of **1** and **4**, the intracellular copper level increased by 135- and 50-fold, respectively, whereas **2**, **3**, **5**, and **6** did not change the accumulation of intracellular copper. It is known that copper intake is mediated by membrane transporter proteins such as Ctr1p, Ctr3p, and others and such intake is well controlled [1, 41]. Our unpublished work on the direct effect of the synthesized Cu–$\mathbf{1}_2$ complex showed that the copper complexes have antiproliferative effects comparable to those of their copper mixtures. The proteasome-inhibitory effects were strictly attributed to the complexes with copper. Ligand alone was active against the tumor cells only when they were grown in copper-enriched medium, where an increased level of cellular copper was available to react with the ligand [32]. Incubation of cells with copper only elevated the cellular level of copper slightly, owing to the tight regulation of copper influx by cells. It seemed that the copper transport by **1** and **4** was independent of transporter proteins. This elevation of cellular copper may have significant consequences inside cells.

One of the consequences is the inhibition of human breast cancer cell proliferation by **1**–Cu or **4**–Cu. In contrast, copper mixtures of compounds **2**, **3**, **5**, and **6** did not inhibit cancer cell proliferation. The net accumulation of compounds **2**, **3**, **5**, and **6** to a level similar to that of **1** and **4** was expected owing to their similar membrane permeability and low efflux ratio (Table 1). Our data strongly suggest that the inhibition of cancer cell proliferation requires both the copper binding and cell uptake of the copper complex. The active inhibitor form is most likely **1**–Cu or **4**–Cu complexes.

The inhibition of proliferation of human breast cancer cells by **1**–Cu and **4**–Cu was not due to the passive copper binding. Actually, copper mixtures of **1** and **4** inhibited proteasomal CT-like activity and induced cell death. Losing the capability to bind copper and to cause cellular copper accumulation of analogs **2**, **3**, **5**, and **6** is associated with their failure to inhibit CT-like activity and to induce cell death. Comparing the time courses for **1**–Cu- or **4**–Cu-induced inhibitions of proteasome and DCIS cell proliferation, we found that both processes reached the maximum effect at 8–12 h.

Using an array of chemical probe molecules that mimic the structures of **1** and **4**, but have no copper-binding capability, we revealed that the copper binding by **1** and **4** and the enhancement of cellular copper complex accumulation are prerequisites for their activities to inhibit cancer cell proliferation. Our studies dissected the actions of **1** and **4** into several steps. The process starts with the copper binding by **1** or **4** and then an overwhelming copper transport into cells that generates a 50–135-fold increase in cellular copper (most likely copper complex) accumulation. These copper complexes should then inhibit proteasomal CT-like activity and induce cell death, leading to the inhibition of proliferation of cancer cells. The inactive analogs blocked the very first step in this cancer cell inhibition process.

Both compounds and their copper complexes can enter cells and accumulate inside cells owing to their excellent membrane permeability and low efflux ratio (Table 1). After $CuCl_2$ treatment for 2 days, the addition of analogs of **1** did not cause any cancer cell inhibitory activity, in contrast to the strong inhibition when the **1**–$CuCl_2$ mixture was added. In the former case, the cellular copper concentration is rather

limited and the addition of analogs of **1** only induced the cellular accumulation of inactive analogs of **1** (owing to their high membrane permeability). However, in the latter case, the significant cellular accumulation of **1**–Cu or **4**–Cu was possible. It is likely that only the high cellular level of the copper complexes mediated inhibition of proteasome activity and cell proliferation (Fig. 7).

In summary, **1** and **4** are bioactive copper chelators. When they interacted with copper salt or cellular copper, they inhibited proliferation of cancer cells in vitro and tumor growth in vivo. However, there is controversy owing to reports of copper-independent cell proliferation suppression by these molecules [36]. Using small chemical probe molecules that mimic the structures of **1** and **4**, but have no copper-binding capability, we dissected the complex molecular interaction network and tested the hypothesis that copper binding and transportation of copper into cells are prerequisites for their cancer cell growth-inhibitory activities. Without copper binding, the analogs penetrated the cell membrane and accumulated inside cells in the same way as **1**–Cu or **4**–Cu. These non-copper-binding molecules failed to transport copper into cells. Consequently, the inhibition of proteasomal CT-like activity and cell growth as well as the inducement of cell death, as demonstrated by **1**–Cu and **4**–Cu, were also impaired. The discovery that copper binding and transportation are the structural and functional requirements for the biological activities of **1** and **4** to inhibit cancer cell proliferation demonstrates the utility of small chemical probe molecules in the study of complex cellular processes.

Materials and methods

Materials

1, **3**, **4**, $CuCl_2$, MTT, and DMSO were purchased from Sigma-Aldrich (St. Louis, MO, USA). All the chemicals used for synthesis of **2**, **5**, and **6** were purchased from Acros (Geel, Belgium). Dulbecco's modified Eagle's medium (DMEM)/F12, horse serum, sodium bicarbonate, *N*-(2-hydroxyethyl)piperazine-*N*′-ethanesulfonic acid (HEPES) buffer solution, penicillin, and streptomycin were purchased from Invitrogen (Carlsbad, CA, USA). Fluorogenic peptide substrates (Suc-LLVY-AMC) for the proteasomal CT-like activity assay were from Calbiochem (San Diego, CA, USA). Mouse monoclonal antibody against human PARP was purchased from Biomol International (Plymouth Meeting, PA, USA). Mouse monoclonal antibodies against Bax (B-9) and ubiquitin (P4D1), goat polyclonal antibody against actin (C-11), and secondary antibodies were from Santa Cruz Biotechnology (Santa Cruz, CA, USA). The water used in this study was purified by reverse osmosis on a Milli-Ro followed by ion exchange.

Instruments

UV–vis spectra were recorded using a Shimadzu (Kyoto, Japan) 2550 UV spectrophotometer. Fluorescence spectra were recorded with a Hitachi (Tokyo, Japan) F-4500 spectrofluorimeter. ^{1}H NMR spectroscopy was carried out with a Bruker (Germany) AVANCE 400 nuclear magnetic resonance spectrometer. LC–MS was performed with a Shimadzu system. A C_{18} column (2.0 μm, 2.0 mm × 50 mm) was used for the separation. The mobile phases were methanol and water both containing 0.05% methanoic acid. A linear gradient was used to increase the ratio from 25:75 v/v methanol–water to 100% methanol over 8.0 min at a flow rate of 0.3 mL/min. The UV detection was at 214 nm. Mass spectra were recorded in positive and negative ion mode using electrospray ionization (ESI). Cellular copper content was determined using a Varian (Palo Alto, CA, USA) 715-ES ICP-OES system. A Zeiss (Thornwood, NY, USA) Axiovert 25 microscope with phase contrast was used for cellular morphology studies.

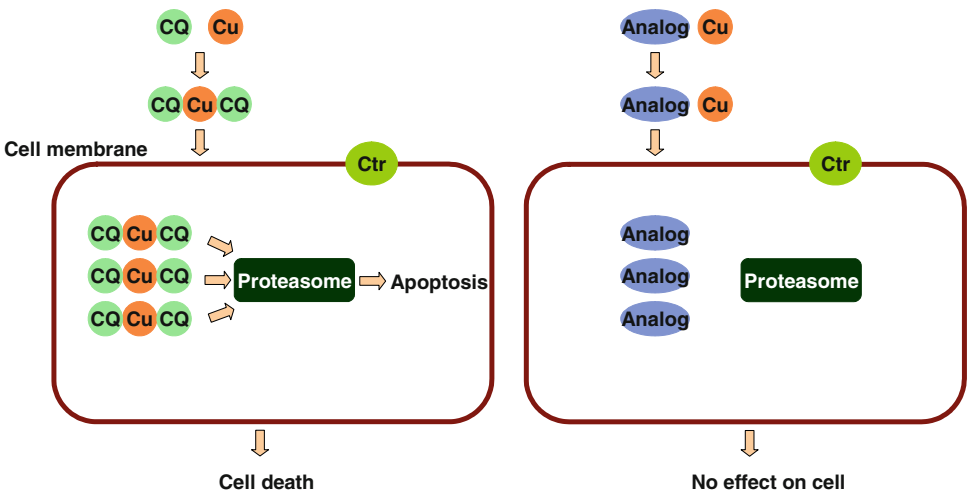

Fig. 7 Working model for the anticancer action of **1** and **4** (*CQ*) (shown as example) and the blockade of such action by non-copper-binding analogs

Synthesis of **2**, **5**, and **6**

1 (0.2 g, 1.38 mmol) was dissolved in dimethylformamide (2 mL). Solid K_2CO_3 (0.55 g) and iodomethane (0.26 mL) were added. The reaction mixture was stirred at room temperature for 24 h. Water (20 mL) was added to stop the reaction, followed by acyl acetate extraction, washing with water, and drying to give **2**. Yield:, 72%, ESI–MS: *m*/*z* 160 ($M + 1$). **5** and **6** were made by the same esterification process as 2.

6. Yield: 60%, ESI–MS: *m*/*z* 194 ($M + 1$).

5. Yield: 87%, ESI–MS: *m*/*z* 320 ($M + 1$).

Determination of Cu–ligand binding constant using UV–vis titration

A methanol solution of $CuCl_2$ (2.5 mM) was titrated into a 3-mL methanol solution of the compound (0.1 mM) in 10-μL increments. The UV spectra were recorded using a UV-2550 UV–vis spectrophotometer.

Cell proliferation assay

The MTT assay was used to measure the effects of the various compounds or compound–copper mixtures on breast cancer cell proliferation. Cells were plated in a 96-well plate and grown to 70–80% confluency, followed by the addition of each compound–copper mixture at the concentrations indicated. After incubation at 37 °C for 24 h, inhibition of cell proliferation was measured using the MTT method.

Measurement of copper accumulation in the breast cancer cells

For copper-uptake measurement, the DCIS cells were plated in 150-mm dishes in DMEM/F12 medium (containing 5% horse bovine serum, 0.029 M sodium bicarbonate, 10 mM HEPES buffer solution, 100 units/mL of penicillin, and 100 μg/mL of streptomycin). When the plates were 80% confluent, 10 μM compound–$CuCl_2$ mixture was added, and the plates were incubated at 37 °C in 5% CO_2 for various times. After they had been rinsed three times with ice-cold phosphate-buffered saline, the cells were harvested by digesting them with trypsin–EDTA scraping, followed by centrifugation for 5 min at 1,400 rpm and 4 °C. The resulting pellet was dissolved in 70% nitric acid at 65 °C for at least 4 h. Samples were diluted to 5% nitric acid with water and the copper content was determined using a Varian (Palo Alto, CA, USA) 715-ES ICP-OES system.

Parallel artificial membrane permeability assay

This assay is used to analyze the permeability of various compounds on a homogeneous artificial lipid membrane. Six microliters of a 10 mM compound solution in DMSO was applied to each well in a 96-well plate. The compounds were diluted 200-fold in buffer (pH 7.4; pION, Woburn, MA, USA). One hundred and eighty microliters of diluted solution was added to a donor plate (pION, Woburn, MA, USA). A filter plate (acceptor plate; pION, Woburn, MA, USA) containing 200 μL of acceptor sink buffer (pH 7.4; pION, Woburn, MA, USA) was then placed over the donor plate. The plates were incubated at room temperature for 0.5 h with magnetic stirring in individual wells to allow the compounds to cross the membrane. Fractions were collected from both the donor plate and the acceptor plate, and the concentrations were assessed by UV plate spectrometry. Sample preparation, sample analysis, and data processing were fully automated using a Biomek ADME-TOX workstation and the UV-based PAMPA Evolution 96 command software (Beckman Coulter, Fullerton, CA, USA).

Caco-2 permeability assay

High-throughput Caco-2 permeability assay was performed in the 96-well transwell system. The cells were cultured in minimum essential medium containing 20% fetal bovine serum in 75-cm^2 flasks, 100 units/mL of penicillin, and 100 μg/mL of streptomycin and were maintained at 37 °C in a humidified incubator with an atmosphere of 5% CO_2. The Caco-2 cells were seeded onto inserts of a 96-well plate at a density of 0.165×10^5 cells per insert and cultured in minimum essential medium containing 10% fetal bovine serum for 21 days. The integrity of the monolayer was checked by transmembrane electric resistance measurements.

Each cultured monolayer on the 96-well plate was washed twice with Hank's balanced salt solution/HEPES (10 mM, pH 7.4). The permeability assay was initiated by the addition of each compound solution (50 μM) into inserts (apical side) or receivers (basolateral side). The Caco-2 cell monolayers were incubated for 2 h at 37 °C. Fractions were collected from receivers (if apical to basal permeability) or inserts (if basal to apical permeability), and the concentrations were assessed by ultraperformance LC–MS (Waters, Milford, MA, USA).

The apical side to basolateral side (or basolateral side to apical side) apparent permeability coefficients (Papp, nm/s) of each compound were calculated using the equation, $\text{Papp} = \mathrm{d}Q/\mathrm{d}t \times 1/AC_0 \times 10$. The flux of a drug across

the monolayer is dQ/dt (μmol/s). The initial drug concentration on the apical side is C_0 (μM). The surface area of the monolayer is A (cm^2). The efflux ratio was defined as the ratio of the basolateral side to the apical side apparent permeability coefficient and the apical side to the basolateral side apparent permeability coefficient.

Cell cultures and whole cell extract preparation

Human breast cancer DCIS cells were grown in DMEM/F12 supplemented with 5% (v/v) horse bovine serum, 0.029 M sodium bicarbonate, 10 mM HEPES buffer solution, 100 units/mL of penicillin, and 100 μg/mL of streptomycin, at 37 °C in a humidified incubator with an atmosphere of 5% CO_2. The whole cell extract was prepared as previously described [18]. Briefly, cells were washed twice with phosphate-buffered saline and homogenized in a lysis buffer [50 mM tris(hydroxymethyl)aminomethane–HCl, pH 8.0, 150 mM NaCl, 0.5% NP40]. After they had been rocked for 20 min at 4 °C, the mixtures were centrifuged at 12,000g for 15 min and the supernatants were collected as whole cell extracts.

Proteasome activity assay

Breast cancer cells were grown to 70–80% confluency, treated as indicated, harvested, and then used for whole cell extract preparation. Proteasomal CT-like activity was assayed as previously described [28]. Briefly, cell lysates (7.5 μg) were incubated with 40 μM fluorogenic substrate for proteasomal CT-like activity for 2 h at 37 °C in 100 μL of assay buffer [50 μM tris(hydroxymethyl)aminomethane–HCl, pH 7.5]. After incubation, production of hydrolyzed 7-amino-4-methylcoumarin groups was measured using a Victor^3 multilabel counter (PerkinElmer, Boston, MA, USA). Statistical analysis was performed using SigmaPlot 8.0.

Western blot analysis

Breast cancer DCIS cells were treated as already described. Cell lysates (50 μg) were separated by sodium dodecyl sulfate polyacrylamide gel electrophoresis and transferred to a nitrocellulose membrane, followed by visualization using an enhanced chemiluminescence kit (Amersham Biosciences, Piscataway, NJ, USA), as previously described [29].

Acknowledgments This work was supported by Shandong University, the American Lebanese Syrian Associated Charities (ALSAC), and St. Jude Children's Research Hospital (B.Y.)., and research funds from the Karmanos Cancer Institute of Wayne State University (Q.P.D.), the Department of Defense Breast Cancer Research Program (W81XWH-04-1-0688, DAMD17-03-1-0175; Q.P.D.) and the National Cancer Institute (1R01CA120009, 1R21CA139386-01; Q.P.D.).

References

1. Labbe S, Thiele DJ (1999) Trends Microbiol 7:500–505
2. Maverakis E, Fung MA, Lynch PJ, Draznin M, Michael DJ, Ruben B, Fazel N (2007) J Am Acad Dermatol 56:116–124
3. Geraki K, Farquharson MJ, Bradley DA (2002) Phys Med Biol 47:2327–2339
4. Nayak SB, Bhat VR, Upadhyay D, Udupa SL (2003) Indian J Physiol Pharmacol 47:108–110
5. Diez M, Arroyo M, Cerdan FJ, Munoz M, Martin MA, Balibrea JL (1989) Oncology 46:230–234
6. Yoshida D, Ikeda Y, Nakazawa S (1993) J Neurooncol 16:109–115
7. Eatock MM, Schatzlein A, Kaye SB (2000) Cancer Treat Rev 26:191–204
8. Fox SB, Gasparini G, Harris AL (2001) Lancet Oncol 2:278–289
9. Brewer GJ (2001) Exp Biol Med (Maywood) 226:665–673
10. Adsule S, Barve V, Chen D, Ahmed F, Dou QP, Padhye S, Sarkar FH (2006) J Med Chem 49:7242–7246
11. Brewer GJ, Dick RD, Grover DK, LeClaire V, Tseng M, Wicha M, Pienta K, Redman BG, Jahan T, Sondak VK, Strawderman M, LeCarpentier G, Merajver SD (2000) Clin Cancer Res 6:1–10
12. Redman BG, Esper P, Pan Q, Dunn RL, Hussain HK, Chenevert T, Brewer GJ, Merajver SD (2003) Clin Cancer Res 9:1666–1672
13. Landis-Piwowar KR, Milacic V, Chen D, Yang H, Zhao Y, Chan TH, Yan B, Dou QP (2006) Drug Resist Updates 9:263–273
14. Orlowski RZ, Dees EC (2003) Breast Cancer Res 5:1–7
15. Ciechanover A (1998) EMBO J 17:7151–7160
16. Seemuller E, Lupas A, Stock D, Lowe J, Huber R, Baumeister W (1995) Science 268:579–582
17. Kisselev AF, Callard A, Goldberg AL (2006) J Biol Chem 281:8582–8590
18. An B, Goldfarb RH, Siman R, Dou QP (1998) Cell Death Differ 5:1062–1075
19. Lopes UG, Erhardt P, Yao R, Cooper GM (1997) J Biol Chem 272:12893–12896
20. Nordenberg J, Novogrodsky A, Beery E, Patia M, Wasserman L, Warshawsky A (1990) Eur J Cancer 26:905–907
21. Shen AY, Wu SN, Chiu CT (1999) J Pharm Pharmacol 51:543–548
22. Moret V, Laras Y, Cresteil T, Aubert G, Ping DQ, Di C, Barthelemy-Requin M, Beclin C, Peyrot V, Allegro D, Rolland A, De Angelis F, Gatti E, Pierre P, Pasquini L, Petrucci E, Testa U, Kraus JL (2009) Eur J Med Chem 44:558–567
23. Deraeve C, Boldron C, Maraval A, Mazarguil H, Gornitzka H, Vendier L, Pitie M, Meunier B (2008) Chemistry 14:682–696
24. Martirosyan AR, Rahim-Bata R, Freeman AB, Clarke CD, Howard RL, Strobl JS (2004) Biochem Pharmacol 68:1729–1738
25. Dou QP, Li B (1999) Drug Resist Updates 2:215–223
26. Adams J (2003) Drug Discov Today 8:307–315
27. Ding WQ, Liu B, Vaught JL, Yamauchi H, Lind SE (2005) Cancer Res 65:3389–3395
28. Daniel KG, Chen D, Orlu S, Cui QC, Miller FR, Dou QP (2005) Breast Cancer Res 7:R897–R908
29. Chen D, Peng F, Cui QC, Daniel KG, Orlu S, Liu J, Dou QP (2005) Front Biosci 10:2932–2939
30. Li L, Xu B (2008) Tetrahedron 64:10986–10995
31. Bevan JA, Graddon DP, McConnell JF (1963) Nature 199:363
32. Daniel KG, Gupta P, Harbach RH, Guida WC, Dou QP (2004) Biochem Pharmacol 67:1139–1151

33. Chen D, Cui QC, Yang H, Barrea RA, Sarkar FH, Sheng S, Yan B, Reddy GP, Dou QP (2007) Cancer Res 67:1636–1644
34. Treiber C, Simons A, Strauss M, Hafner M, Cappai R, Bayer TA, Multhaup G (2004) J Biol Chem 279:51958–51964
35. Mao X, Li X, Sprangers R, Wang X, Venugopal A, Wood T, Zhang Y, Kuntz DA, Coe E, Trudel S, Rose D, Batey RA, Kay LE, Schimmer AD (2009) Leukemia 23:585–590
36. Filiz G, Caragounis A, Bica L, Du T, Masters CL, Crouch PJ, White AR (2008) Int J Biochem Cell Biol 40:1030–1042
37. Vaira MD, Bazzicalupi C, Orioli P, Messori L, Bruni B, Zatta P (2004) Inorg Chem 43:3795–3797
38. Ferrada E, Arancibia V, Loeb B, Norambuena E, Olea-Azar C, Huidobro-Toro JP (2007) Neurotoxicology 28:445–449
39. Pink JJ, Wuerzberger-Davis S, Tagliarino C, Planchon SM, Yang X, Froelich CJ, Boothman DA (2000) Exp Cell Res 255:144–155
40. Cvek B, Milacic V, Taraba J, Dou QP (2008) J Med Chem 51:6256–6258
41. Harris ED (2000) Annu Rev Nutr 20:291–310